Detection of Emotional Sensitivity Using fNIRS Based Dynamic Functional Connectivity

Tong Boon Tang, *Senior Member, IEEE*, Jie Sheng Chong, Masashi Kiguchi, Tsukasa Funane, and Cheng-Kai Lu, *Senior Member, IEEE*

***Abstract*—In this study, we proposed an analytical framework to identify dynamic task-based functional connectivity (FC) features as new biomarkers of emotional sensitivity in nursing students, by using a combination of unsupervised and supervised machine learning techniques. The dynamic FC was measured by functional Near-Infrared Spectroscopy (fNIRS), and computed using a sliding window correlation (SWC) analysis. A *k*-means clustering technique was applied to derive four recurring connectivity states. The states were characterized by both graph theory and semi-metric analysis. Occurrence probability and state transition were extracted as dynamic FC network features, and a Random Forest (RF) classifier was implemented to detect emotional sensitivity. The proposed method was trialled on 39 nursing students and 19 registered nurses during decision-making, where we assumed registered nurses have developed strategies to cope with emotional sensitivity. Emotional stimuli were selected from International Affective Digitized Sound System (IADS) database. Experiment results showed that registered nurses demonstrated single dominant connectivity state of task-relevance, while nursing students displayed in two states and had higher level of task-irrelevant state connectivity. The results also showed that students were more susceptive to emotional stimuli, and the derived dynamic FC features provided a stronger discriminating power than heart rate variability (accuracy of 81.65% vs 71.03%) as biomarkers of emotional sensitivity. This work forms the first study to demonstrate the stability of fNIRS based dynamic FC states as a biomarker. In conclusion, the results support that the state distribution of dynamic FC could help reveal the differentiating factors between the nursing students and registered nurses during decision making, and it is anticipated that the biomarkers might be used as indicators when developing professional training related to emotional sensitivity.**

***Index Terms*—Emotional sensitivity, dynamic functional connectivity, functional Near-Infrared Spectroscopy, Random Forest, heart rate variability.**

Manuscript received October 30, 2020; revised March 31, 2021; accepted May 5, 2021. Date of publication May 10, 2021; date of current version May 18, 2021. This work was supported by the Ministry of Higher Education, Malaysia, under Higher Institution Centre of Excellence (HICoE) Scheme awarded to Centre for Intelligent Signal and Imaging Research (CISIR). *(Corresponding authors: Tong Boon Tang; Jie Sheng Chong.)*

Tong Boon Tang, Jie Sheng Chong, and Cheng-Kai Lu are with the CISIR, Universiti Teknologi PETRONAS, Bandar Seri Iskandar 32610, Malaysia (e-mail: tongboon.tang@utp.edu.my; cjs_chong@hotmail.com).

Masashi Kiguchi and Tsukasa Funane are with the Center for Exploratory Research, Research and Development Group, Hitachi, Ltd., Tokyo 185-8601, Japan.

This article has supplementary downloadable material available at https://doi.org/10.1109/TNSRE.2021.3078460, provided by the authors.

Digital Object Identifier 10.1109/TNSRE.2021.3078460

I. Introduction

According to the Appraisal Theory of Emotion [1], emotion is a psycho-physiological process arising from the evaluation of an event. Wansink and Sobal showed that humans may make more than 200 decisions daily just only on food [2]. The change of emotion, however, will result in the meaning of a message being twisted or making an unusual decision [3]. The primary evaluation of emotion based on the facial expression, tone of human voice or self-assessment questionnaire are subjective and susceptive to language or habit bias, resulting in a low recognition accuracy [4]. Humans can pretend or hide their true emotion via their voluntary action. Besides, the diagnosis of human's neurological condition such as depression requires interview and is expert dependent [5]. Such human based recognition of emotion might inherent human error. Thus, the emotion recognition techniques now involve physiological signal measurements such as cardiac response, electromyogram and galvanic skin response [6], [7].

Recent neuroimaging studies in functional magnetic resonance imaging (fMRI) [8], [9] have produced some promising results to better explain the neural activities in emotional processing. Findings showed that the emotional response is being reflected in neural activities or functional connectivity (FC) between multiple brain regions such as lateral prefrontal cortex (PFC), hippocampus, cingulate cortex, and amygdala. This provided a hint on how we might detect emotional state by inspecting the change of activities in the central nervous system and peripheral nervous system, which are involved in emotional processing [10]. Coupled with machine learning (ML), neuroimaging modalities such as electroencephalography (EEG) and fMRI have gained popularity in predicting humans' emotional states [11], [12].

One potential application of emotion recognition techniques is in professional training. While it is not new, high nursing student dropout rate is a global concern [13]. Although the reasons for leaving could be complicated and probably inter-linked [14], lack of stress coping strategies has been identified as a contributing issue [15]. In particular, the clinical part of the nursing education is found to be more stressful than the theoretical part [16]. Studies have suggested the need of academic authorities to provide necessary training on effective coping strategies to nursing students [17]–[19]. However, little is known about how aforementioned emotion recognition techniques could assist in the training of stress coping strategies.

This study proposes to exploit functional Near Infrared Spectroscopy (fNIRS) to detect emotional sensitivity. Emotional sensitivity can be defined as a lower threshold to respond to emotional stimuli, or a higher probability of experiencing stimuli as emotional [20]. Our previous study [21] showed that nursing students had a higher correlation between static FC coherence and behavioral accuracy in an affective task, as compared with a neutral task. Yet, brain connectivity is inherently dynamic, especially when involving task-evoked neural activities [22]. A recent fNIRS study [23] investigated emotional dysregulation in children with attention-deficit/hyperactivity disorder (ADHD), and examined them using cortical activation (i.e., hemodynamic concentration changes). However, Sutoko *et al* [24] demonstrated that dynamic FC could provide a better performance than hemodynamic activation in screening ADHD children whom often display lack of emotion recognition [25]. Hence, we hypothesize that dynamic FC network features could provide useful biomarkers to detect emotional sensitivity among nursing students and registered nurses, where we assumed registered nurses have developed strategies to ameliorate emotional sensitivity. We further propose an analytical framework, a combination of unsupervised and supervised ML to identify dynamic FC features as new emotion sensitivity neural markers, and compare the results against a benchmark method (heart rate variability, HRV). This work is also the first in demonstrating the stability of fNIRS based dynamic connectivity state feature as a biomarker of emotional sensitivity.

II. Methodology

In this section, we first explain about the designed experiment involving a group of nursing students and a group of registered nurses. Then we describe the proposed method which comprises data analysis, unsupervised clustering analysis, and supervised machine learning modules. Network characterization and statistical analysis are included to validate the experiment results. We assess our hypothesis by comparing: 1) the affective effects on dynamic FC of nurses and students, and 2) the discriminating power of dynamic FC and HRV as input features in detecting emotional sensitivity.

A. Designed Experiment

1) Participant Demographics: Two groups of right-handed and healthy nursing members comprising 19 registered nurses, abbreviated as nurses (Edinburgh Handedness Inventory [26] scale = 92.11 ±10.10, age = 30.44 ±3.20 years old, working experience = 8.32 ±3.04 years) and 40 nursing students, abbreviated as students (Edinburgh Handedness Inventory scale = 87.18 ±14.30, age = 19.48 ±1.04 years old, internship experience = 2.70 ±0.41 years) were recruited for this experiment. None of the subjects had a history of cardiovascular or psychiatric disease. They were also not allowed smoking, exercising and taking any caffeine and alcohol 3 hours before the experiment. One student who violated the requirements was excluded from the analysis. This study was approved by the ethics committees of Universiti Kuala Lumpur Royal College of Medicine Perak with approval number of UniKL-RCMP/MREC/2018/018. All subjects gave written consent prior to the experiment and the experiment was carried out in accordance with the Declaration of Helsinki.

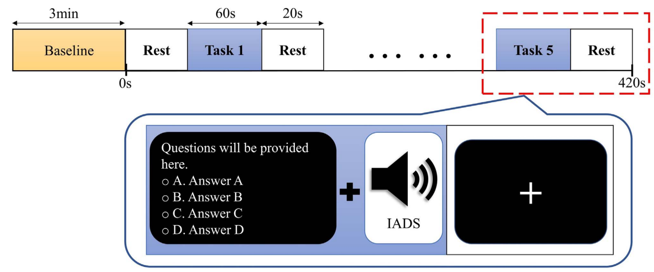

Fig. 1. Task paradigm for designed experiment.

2) Data Acquisition: A dual-wavelength (695 nm and 830 nm) multichannel continuous wave OT-R40 fNIRS system (Hitachi Medical Corporation, Japan) was employed to measure the cerebral hemodynamic activities at the temporal resolution of 0.1 s (10 Hz). The 52-channel probes (consisting of 17 sources and 16 detectors) with a source-detector distance of 3 cm was deployed as 3 × 11 optodes configuration. The optodes were setup on PFC and temporal areas along the T4-Fpz-T3 positions in line with the international 10-20 system [27]. A simultaneous measurement (sampling rate: 200 Hz) of photoplethysmographic (PPG) signals for HRV analysis was recorded using a Nellcor DS-100A ear clip sensor connected to AFE4490SPO2EVM Evaluation Board (Texas Instruments Inc, Dallas, Texas). The PPG was selected as its measurement was correlated to electrocardiogram signals [28].

3) Experiment Protocol: The selection of emotional stimuli was based on the Self-Assessment Manikin (SAM) 9-point rating in the emotional circumplex model [29], considering two independent neurophysiological dimensions: valance and arousal. From the model, ten affective (case) sound clips (negative valence: 2.147 ±0.473; high arousal: 7.388 ±0.494) and ten neutral (control) sound clips (neutral valence: 5.197 ±0.720; medium arousal: 4.560 ±0.380) were retrieved from the International Affective Digitized Sounds system (IADS) [30].

This experiment was designed in a counterbalanced manner to avoid the order effect, where each participant had to attend two sessions (one with affective stimuli and the other with neutral stimuli). Participants were randomly assigned to each session where 50% would be under affective stimuli at one time. Participants were seated in front of a monitor. As shown in Fig. 1, a 3-minute baseline establishment was conducted prior to the experiment. The experiment began with 20 seconds of rest followed by five alternating trials of task and rest. While resting, subjects were asked to relax by concentrating on the displayed white cross. During the task, up to five four-choice nursing-scenario-study questions were presented successively on the screen. The difficulty level of the questions in both sessions were standardized based on the Bloom's taxonomy [31]. Within 60 seconds, subjects

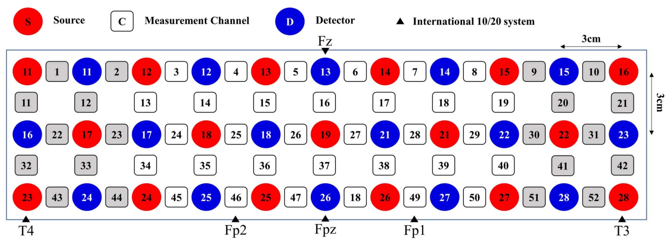

Fig. 2. Source-Detector pair configuration based on the international 10/20 system.

were to answer promptly and complete as many questions as possible. The total correct attempt, accuracy (correct attempt over the total attempt) and response time were recorded for statistical analysis. Simultaneously, subjects were listening to the acoustic stimulus played by a speaker without knowing the valance and arousal ratings. After six weeks' time, all subjects would attend the second session of the experiment with emotional stimuli different from their own first session.

B. Proposed Method

The proposed method comprises seven modules, as described in Fig. 3. The collected fNIRS signals were initially preprocessed and the subjects' dynamic FC constructed by sliding window correlation (SWC). The extracted dynamic FC matrices were analyzed using unsupervised clustering analysis to identify key recurring states. These states were characterized by graph theory analysis and semi-metric analysis. In parallel, the dynamic FC properties were extracted as features before fed into a Random Forest classifier and quantified its performance for comparison between the two groups of participants.

1) Data Preprocessing: In this study, the fNIRS signal preprocessing was conducted using MATLAB (MathWorks Inc., Natick, MA). First of all, as shown in Fig. 3 we applied wavelet-based motion correction [32] on the optical density of dual-wavelength fNIRS signals to remove the artifact due to body motion. By converting to oxygenated hemoglobin concentration change (ΔHbO) and deoxygenated hemoglobin concentration change (ΔHbR) using Modified Beer-Lambert Law, the high-frequency noise (i.e., cardiac pulsation and respiration effect) and baseline drift were removed by 4th order Butterworth band-pass filter on frequency band between 0.01 Hz to 0.2 Hz and first order polynomial baseline fitting respectively. Subsequently, we performed the hemodynamic modality separation (HMS) method [33] to eliminate systemic physiological fluctuations including skin blood flow. As the HMS method extracted the functional signal components based on the assumption of the linear relationship between ΔHbO and ΔHbR, the generated FC maps would eventually be the same for both signal types. Therefore, we only selected the functional ΔHbO signals as the backbone signals.

2) Dynamic FC: To capture the dynamic FC, we performed the SWC method [22], [34]. Based on previous studies [35], [36], we selected a fixed window size of 30 s to provide a good trade-off between the false fluctuation and over-smoothing. With a step size of 1 s, we captured the channel-pairwise correlation, producing (channels $\times$ channels $\times$ sliding time) dynamic FC matrices for each subject, where sliding time is the difference between total signal times and window size. After that, we concatenated all subjects' dynamic FC matrices, resulting in a 2D matrix of all inter-channel correlation vectors $\times$ sliding time across all subjects.

3) Unsupervised Clustering Analysis: To identify the recurring connectivity states, unsupervised k-means clustering algorithm was applied to partition the 2D matrices into k clusters of connectivity states without any label. However, it is important to identify the suitable number of clusters prior to execution. Excessively greater or smaller cluster number would lead to mismatch or over-fitting in clustering, respectively. Thus, to identify the optimal k, we executed k-mean clustering analysis on the concatenated FC matrices by varying the cluster number, k from 1 to 10. Thereafter, Elbow method was applied to determine the bend (or elbow) of the curve with the minimum intra-cluster variation based on within-cluster sum of square (WSS) Euclidean distance [37].

4) Network Characterization: Based on the connectivity states, we could observe the information transfer between regions in the network using the generated correlation matrices. To characterize each generated connectivity state, we employed not only graph theory analysis but also the semi-metric analysis as the shortest path is not always the direct distance. The semi-metric permits higher level of information sharing through circuitous paths and these network redundancies are not considered in conventional graph theory. Semi-metricity has also been identified as one of the main symptoms of neurodevelopment disorder (autism) and post-traumatic stress disorder (emotional processing) [38], [39].

a) Graph theory: As the first step of network quantification, we performed a typical graph theory approach [40]. The network topology analysis was calculated using Brain Connectivity Toolbox (BCT) [41]. First, the constructed FC networks were then submitted to remove spurious or weak connectivity by thresholding method. We selected proportional (sparsity-based) thresholding rather than absolute (correlation-based) thresholding because of its higher stability to assess complex network FC in previous research [42]. The FC networks were thresholded across all possible thresholds of densities, K, which could be defined as the proportion of total existing edges relative to total number of possible of edges in the networks. To avoid the arbitrary of selecting thresholds, we selected the density thresholds range $0.1 < K < 0.5$ with the step size of 0.001 of the FC networks. Specifying the thresholds range could avoid the brain network going random at higher cost (when D approaching 0.5) and prevent excess elimination of edges due to insufficient cost [43]. Within the thresholds range, the brain networks were binarized into unweighted and undirected graphs by setting suprathreshold and subthreshold correlation values 1 and 0 respectively.

In this analysis, we focused on topological network efficiency, one of the common quantifying tools to evaluate the capability of information exchange in FC network. From the thresholded functional network, we computed the network topology efficiencies including global efficiency, E_{global} and local efficiency, E_{local} as shown in equation (1) and (2).

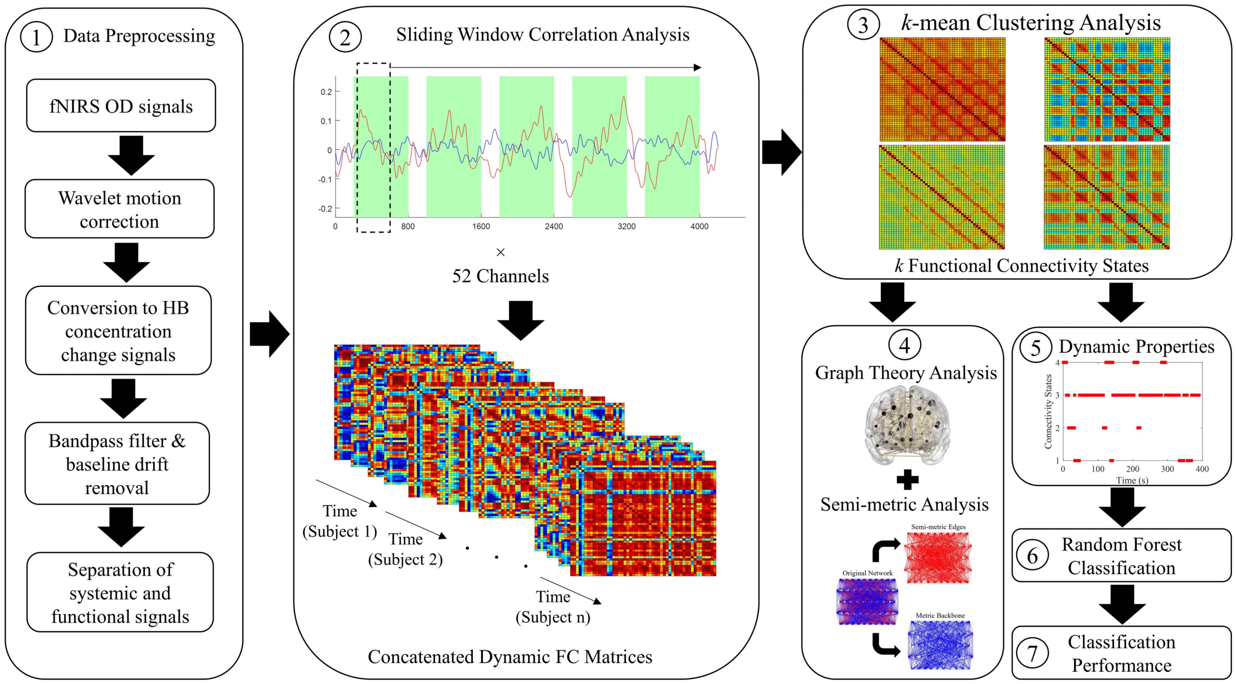

Fig. 3. Proposed method to detect emotional sensitivity.

The E_{global} is defined as the inverse of the harmonic mean of the shortest path length within the whole network [44]. It measures the capacity of global transmission of information across the networks. It can be derived from the following:

$$E_{global} = \frac{1}{N(N-1)} \sum_{j \neq i \in G} \frac{1}{d_{ij}} \tag{1}$$

where d_{ij} the shortest path length between node i and j; N represents the total node number in the network, G. The E_{local} of a network is the average local efficiencies of each node [40] and the local efficiency of each node, $E_{local}(G)$ can be calculated using Eq. (2).

$$E_{local}(G) = \frac{1}{N} \sum_{i \in G} E_{global}(G_i) \tag{2}$$

where the global efficiency of G_i each subgraph G comprising node i with its first neighbors represents the local efficiency of each node. Besides determining the effectiveness of information transfer between node i and its nearest neighbor nodes, $E_{local}(G)$ provides the estimation of nodal defect tolerance for the neighboring nodes around node i. Across the specified threshold range, the representations of E_{global} and E_{local} were computed as the area under the curve (AUC).

b) Semi-metric analysis: Besides graph theory, we also conducted an emerging semi-metric analysis [45] as another network metric. The weighted and undirected correlation matrix graph was converted to a distance graph using a distance conversion function [46] in Eq. (3):

$$d'_{ij} = \frac{1}{r_{ij}} - 1 \tag{3}$$

where d' denotes the distance function of r_{ij}, correlation weight between nodes i and j.

From the distance graph, we computed the ratio of semi-metricity, s_{ij}, defining the proportion of direct distance to the circuitous path between two nodes, as computed in Eq. 4 [45]:

$$s_{ij} = \frac{d'_{ij}}{d_{ij}} \tag{4}$$

where d_{ij} is defined as the shortest direct or circuitous path between nodes i and j generated by path finding algorithm (i.e., Johnson's Algorithm [47]).

Ultimately, the semi-metric percentage (SMP) was calculated for each FC matrix as [45]:

$$SMP = \frac{\sum_{i,j} s_{ij} > 1}{E} \tag{5}$$

where E is the total number of direct connections in the original network. The SMP quantifies semi-metric behavior of the brain network, reflecting a higher level of synchronous and dispersal connection between brain regions. Such network behavior has been associated to the hyper-connectivity in PFC areas during emotional processing such as anxiety and stress [48], [49].

5) Dynamic FC Feature Extraction: From the generated dynamic FC matrices, we identified two different time-varying properties: occurrence probability and state transition. To assess the task effect, the 20-s resting state data for each trial was excluded from the calculation.

a) Occurrence probability: From each subject FC sliding time point, the occurrence probability [34] was computed as the ratio of total occurrence of a particular connectivity state to the total task-relevant sliding time:

$$Occurrence\ Probability\ (k) = \frac{\sum_{t=1}^{T} (S(t) = k)}{T} \tag{6}$$

where k denotes a connectivity state number; $S(t)$ indicates the connectivity states at time point t whereas T represents the total task-relevant period.

b) States transition: The number of transitions of one state to its subsequent state was calculated for each connectivity state. Afterward, we computed the state transition in percentage which is defined as the number of state transition over the total task-relevant period. A subject-wise (states $\times$ states) transition map was generated.

6) Random Forest Classification: Random Forest (RF) is formed by ensembles of classifiers. The RF randomly generates bootstrapped training data sets to enhance classification and preserves the benefits of decision trees (DT). RF was selected as when dealing with limited sample size, it provides solution to 1) overcome weak classification; 2) be robust against over-fitting; 3) be independent to data distribution; 4) manage to handle outliers [50], [51].

The classification function of RF was extracted from Classification Learner Tool in MATLAB (MathWorks Inc., Natick, MA). The concept of RF was dependant on a collection of DT classifiers which casts a vote for each predictor's variables [50]. At the beginning, RF followed two steps of random selection to construct multiple DTs. In the first step, by using bootstrap aggregating (bagging) method, the classifier was trained by using a set of boostrapped data, which is randomly chosen from the original data. Next, each node of the DT was randomly chosen from a subset of variables prior to splitting. The best feature was selected to maximize the learning accuracy by setting the maximum number of splits at default value of 77 (maximum observation number - 1).

Due to the limited sample features in this study, there would be a risk of overfitting. Therefore, the k-fold (10-fold) cross-validation was applied on the data features. First, the two dynamic FC properties of each connectivity state (occurrence probability and transition stability) were selected as the features of classification. The trend of the features was confirmed by assessing the previous paired t-test analysis and the training of features were then repeated for 10 iterations separately among two sample groups to split the k-fold in a different manner. The same classification method was repeated by applying on the HRV features ($RMSSD$ and $SDNN$) together as inputs.

7) Performance Analysis: In the performance analysis, we initially examined the connectivity state(s) that would provide the best emotional state classification performance. To achieve the optimal features selection, we further included all the possible connectivity states features, which identified the significant emotional change, as the input of classification. The subsequent analysis was aimed to compare the discriminating power between dynamic FC features and the conventional HRV features ($RMSSD$ and $SDNN$, simultaneously). The classification performance of HRV and the dynamic FC features were identified based on the area under receiver operating characteristic curve (ROC), classification accuracy, sensitivity and specificity. The classification accuracy was computed as the percentage of true classification (affective task as case) over the total classification samples and the area under ROC were then constructed as the true positive rate against the false positive rate. From the ROC, we estimated the sensitivity and specificity of the classification. The area under ROC was also evaluated with varying a threshold ranged from 0 to 1 [52].

C. HRV Analysis

The current definition of emotion is the strong feeling accompanied by physiological and behavioral changes in the body. HRV has been a reliable biomarker in recognizing emotional states based on the evaluation of the autonomic nervous system responses [7]. To benchmark the proposed dynamic FC, we evaluated the physiological change – HRV using root mean square of successive differences between normal heartbeats (*RMSSD*) and standard deviation of NN intervals (*SDNN*). HRV analysis was executed using the HRVTool v1.04 (https://github.com/MarcusVollmer/HRV) [53] running in MATLAB (MathWorks Inc., Natick, MA). Several preprocessing techniques including moving average filter, NN interval [54] and artifacts elimination [53] were conducted to generate clean NN-intervals signals. From the preprocessed signals, we computed HRV *RMSSD* and *SDNN* using the Eq. 7 and Eq. 8:

$$RMSSD = \sqrt{\frac{1}{n-1}\sum_{i=1}^{n-1}(NN_{i+1} - NN_i)^2} \tag{7}$$

$$SDNN = \sqrt{\frac{1}{n-1}\sum_{i=1}^{n}(NN_i - \overline{NN})^2} \tag{8}$$

where NN_i is the time intervals between successive beats and $\overline{NN}$ indicates the mean of NN intervals.

D. Statistical Analysis

For each network quantifying index (E_{global}, E_{local} and SMP), we compared the statistical differences among the four connectivity states by conducting one-way Analysis of Variance (ANOVA). The following multiple comparison analysis was conducted with the correction of false discovery rate (FDR) [55] at desired q-level (FDR-corrected $p = 0.05$). We also assessed the emotional effect and group effect on the dynamic properties using pairwise comparisons with FDR correction.

In the HRV analysis, one-sample t-test was used separately among students and nurses to evaluate the emotional state effect on *RMSSD* and *SDNN*.

III. Results

A. Selection of Optimal Cluster Number

Based on the Elbow method, the curve of WSS distance against cluster number is generated and displayed in Supplementary Fig. S1. The optimal cluster was identified as the cluster point (from $k = 1$ to 10) with the longest perpendicular distance to a linear line (dotted straight line in the graph) [56]. In this case, the optimal k is 4.

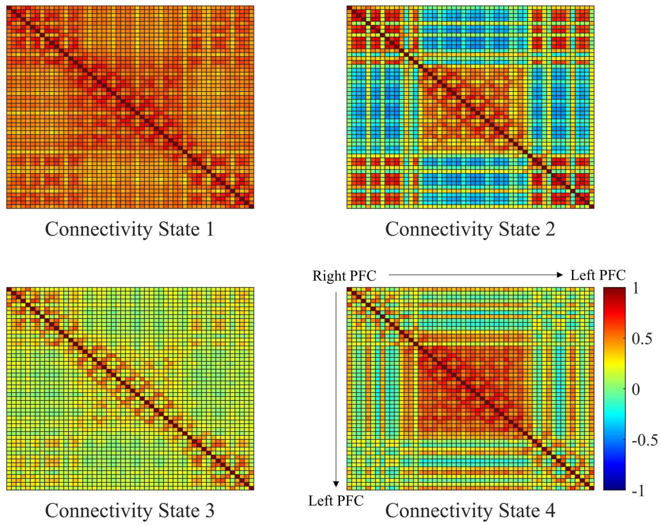

Fig. 4. Generated centroid maps using k-means clustering algorithm. Each colour in the matrices indicates the channel pairwise correlation, r.

B. Unsupervised Clustering Analysis

Using k-means clustering analysis with $k = 4$, four recurring centroid maps were generated as shown in Fig. 4 to represent different patterns of connectivity states. The matrices were re-arranged according to the spatial registration oriented from right to left PFC.

C. Dynamic FC Properties

1) Task Effect on Occurrence Probability: The overall group results revealed that connectivity state 3 (S3) has the highest mean occurrence probability (40.36%), followed by connectivity states 1 (S1) (26.25%), 4 (S4) (20.82%) and 2 (S2) (12.57%). By group, the multiple comparison, adjusted by FDR correction, revealed that the nurses displayed significantly high (FDR-corrected $p < 0.001$) occurrence probability of single state, i.e., S3, as shown in Fig. 5a. No difference between affective and neutral tasks ($p > 0.05$) was observed in the nurse group. In contrast, the student group has task-relevant states (S3 and S4) exhibited significant differently under different task conditions (FDR-corrected $p < 0.05$), as depicted in Fig. 5b. S3 demonstrated significantly higher occurrence probability (FDR-corrected $p = 0.036$) during affective task, while S4 had lower occurrence probability (FDR-corrected $p = 0.036$) than neutral task.

2) Occurrence Probability Between Groups: A multiple comparison was conducted on each connectivity state to compare the group effect on the occurrence probability. The result (refer to Supplementary Table S1) determined that as compared with the nurse group, student group had generally higher level of occurrence probability in S1 (FDR-corrected $p = 0.014$ and $= 0.033$ in affective and neutral task respectively), which has high correlation across all PFC areas [57]. Moreover, nurse group demonstrated significantly higher occurrence probability (FDR-corrected $p = 0.033$ and $= 0.014$ in affective and neutral task respectively) in S3 than that in student group. Among the group comparisons, the largest change was found in S3, where nurses had 18.314% of occurrence probability higher than students during the neutral task.

3) Task Effect on State Transition: The results of another dynamic FC property – state transition were tabulated in matrix form (refer to Supplementary Fig. S2). From the transition matrices, low transition percentages between different states (less than 7%) were found among all sample groups. On the other hand, subjects tended to exhibit high percentage of time being at the same state, also defined as transition stability. The dominant transition stability was found in S3 (nurses: affective = 48.83% and neutral = 47.46%; students: affective = 36.41% and neutral = 28.29%).

When evaluated with the statistical analysis, the state transition was significantly different between affective and neutral tasks for students in S3 (FDR-corrected $p = 0.039$) and S4 (FDR-corrected $p = 0.039$). No significant change between the two tasks for nurses was found in similar S3 and S4 ($p \geq 0.626$).

4) State Transition Between Groups: Based on the multiple comparison in Supplementary Table S1, we observed a significantly higher transition stability in S1 (FDR-corrected $p = 0.019$ and $= 0.026$ in affective and neutral task respectively) in student group that that in nurse group. However, a lower transition stability in S3 (FDR-corrected $p = 0.032$ and $= 0.014$ in affective and neutral task respectively) was observed in the student group as compared with the nurse group. In S3, the nurses demonstrated higher transition stability than students with the largest difference (19.166%) while participating neutral task.

D. Network Characterization

Two different graph theoretical approaches were introduced to characterize each of the four recurring clustered connectivity states, with statistical comparison.

1) Graph Theory: One-way ANOVA was conducted to investigate the connectivity state effect on graph theory analysis. As Mauchly's test indicated the violation of sphericity in the data of E_{global} ($\chi^2(2) = 238.615$, $p < 0.001$) and E_{local} ($\chi^2(2) = 286.299$, $p < 0.001$), Greenhouse-Geisser correction was applied. Significant connectivity state effect was observed in E_{global} [$F(3,115) = 45.498$, $p < 0.001$] and E_{local} [$F(3,115) = 35.168$, $p < 0.001$]. Multiple comparison with the correction of FDR was conducted on the four recurring connectivity states to verify the results of clustering. The experiment results report that S3 has significantly the highest global efficiency (vs S1: FDR-corrected $p < 0.001$; vs S2: FDR-corrected $p < 0.001$; vs S4: FDR-corrected $p = 0.001$) among all connectivity states (see Fig. 6a). S4 was ranked after S3 (FDR-corrected $p < 0.001$) by having higher mean E_{global} than S2 (but not statistically different) and 1 (FDR-corrected $p = 0.016$).

Moving on to another pairwise comparison with FDR correction in Fig. 6b, S2 exhibited the significantly highest local efficiency, E_{local} among all connectivity states (FDR-corrected $p < 0.001$). S3 possessed higher E_{local} than S4 (FDR-corrected $p = 0.002$) and 1 (FDR-corrected $p < 0.001$).

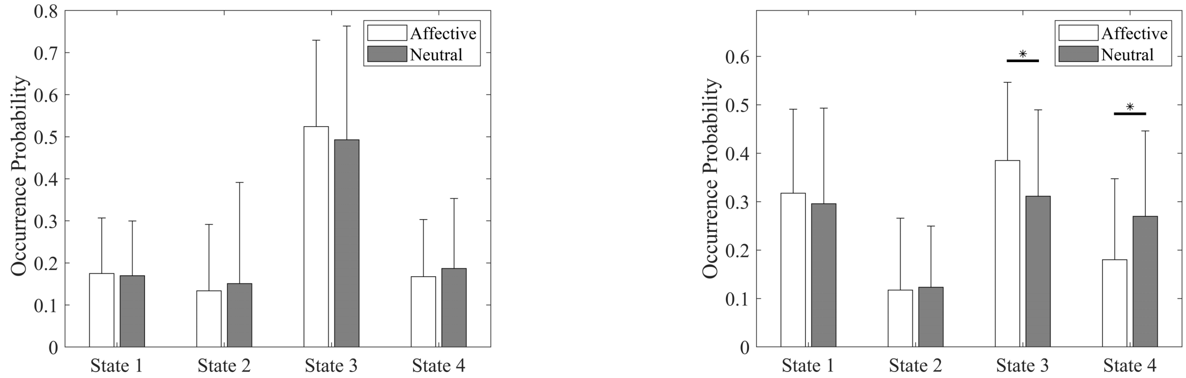

(a) (b)

Fig. 5. Statistical comparison of affective versus neutral states based on the mean occurrence probability of connectivity states across the task-relevant period between (a) Nurses (b) Students. * symbol represents significant level FDR-corrected $p < 0.05$.

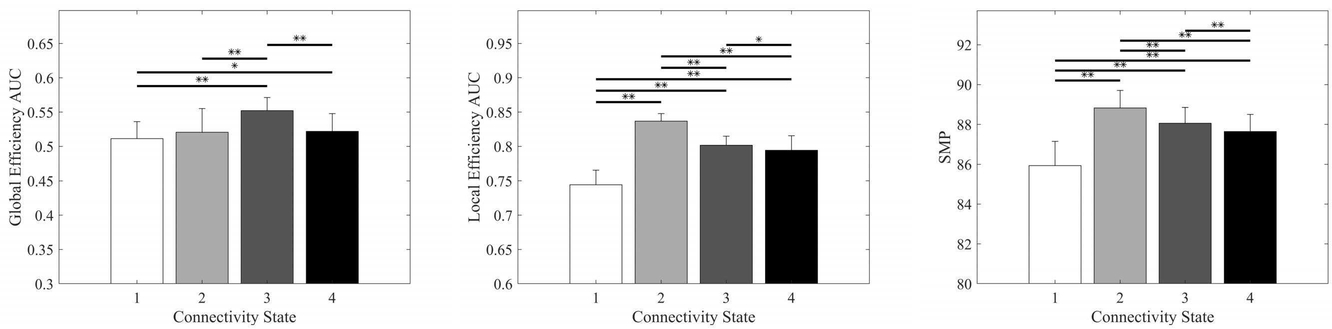

(a) (b) (c)

Fig. 6. Statistical comparison of affective versus neutral states based on the network quantifying techniques: (a) E_{global} (b) E_{local} (c) *SMP*. * and ** symbols indicate significant level FDR-corrected $p < 0.05$ and FDR-corrected $p < 0.001$ respectively.

2) Semi-Metric Analysis: Similar to graph theory analysis, the effect of connectivity state on SMP was studied using one-way ANOVA. Greenhouse-Geisser correction was applied due to the violation of sphericity in Mauchly's test ($\chi^2(2) = 274.728$, $p < 0.001$). The results revealed the main effect of connectivity states to be significant [$F(3{,}115) = 11.250$, $p < 0.001$] and remains significant in the *post hoc* analysis. As illustrated in Fig. 6c, the multiple comparison with FDR-correction demonstrated that a significantly higher mean SMP was observed in S3 (FDR-corrected $p < 0.001$) than that in S1 and S4. S2 demonstrated the highest (FDR-corrected $p < 0.001$) SMP whereas S1 had the lowest (FDR-corrected $p < 0.001$) SMP.

E. HRV Analysis

Statistical comparisons show significantly lower *RMSSD* ($p = 0.0345$) and *SDNN* ($p = 0.0138$) among students in the affective state than that in the neutral state. On the other hand, the nurses did not exhibit any significant change in both *RMSSD* and *SDNN*, under the two different emotional states.

F. Behavioral Performance

The statistical comparisons of the tasks and groups (refer to Supplementary Table S4) were conducted to evaluate the accuracy, correct attempt and response time while attempting the tasks. The findings show that none of the comparison was found to be significant (FDR-corrected $p > 0.05$). However, the average behavioral performance of the students improves by approximately 13% (accuracy: +15.64%, correct attempt: +16.00%, response time: −7.31%) when under the affective condition.

G. Supervised Classification

The RF classification results on the connectivity states among nurses and students, as summarized in Supplementary Table S2, show that the S3 of students Table S2, show that the S3 of students produces the highest single-state emotional state classification performance among all connectivity states. Here, we set the affective state as case. An improvement of the classification was observed in Supplementary Table S3, when both the S3 and S4 were considered as input features to the RF classifier. Two comparison analyses were further carried out as follows. The first comparison was to examine which group has a higher accuracy rate in detecting affective state (as case). We argue that higher accuracy means that the dynamic FC features were more differentiable under affective and neutral emotional states. Conversely, the dynamic FC feature responses to different emotional states would be similar if there was no effect from emotional stimuli; the second comparison was carried out to assess if the proposed dynamic FC features could help detect emotional sensitivity more accurately than the conventional HRV features.

1) Nurses Vs Students: The comparison of the emotional state classification performance based on dynamic FC shows

TABLE I
EMOTIONAL STATE CLASSIFICATION PERFORMANCE BASED ON DYNAMIC FC AND HRV ANALYSIS AMONG STUDENTS AND NURSES

	Dynamic FC		HRV	
	Nurses	**Students**	Nurses	Students
ROC	55.91 (3.81)%	**83.06 (1.72)%**	54.28 (1.97)%	72.81 (1.91)%
Accuracy	55.26 (2.04)%	**81.65 (0.87)%**	53.42 (1.27)%	71.03 (0.90)%
Sensitivity	54.74 (9.18)%	**73.85 (2.02)%**	52.63 (5.55)%	67.44 (2.43)%
Specificity	55.79 (7.14)%	**89.49 (2.25)%**	54.21 (6.10)%	74.62 (1.89)%

that students had higher area under ROC, accuracy, sensitivity and specificity than nurses (refer to Table I). This supports our assumption that the students were more susceptive to emotional change during the affective task, as compared to the nurses.

2) HRV Vs Dynamic FC: The results in Table I show that the dynamic FC (based on both S3 and S4) generated a better emotional state classification performance when compared with cardiac measurements (HRV), in the case of students. In the case of the nurses, we observe a lower classification performance on dynamic FC and HRV, suggesting the dynamic FC does not originate from the emotion management but a result of emotional sensitivity.

IV. DISCUSSION

A. Unsupervised Clustering Analysis

As depicted in Fig. 4, four unique connectivity states were generated by unsupervised clustering analysis. First, S1 demonstrated massively strong association between all regional matrices. This phenomenon could be explained as the global signal that causes widespread of correlation in the brain regions. Besides the residual systemic noise (i.e., local blood circulation), which could not be completely suppressed by denoising method, there might be the arising of the other possible neurovascular components, which required further investigation.

S2 reflected an intrinsic FC network [58]. High correlations were in Default Mode Network (DMN) regions, including medial prefrontal cortex, posterior cingulate cortex and lateral temporal cortex [59]. At the same time, anti-correlation was found between the DMN and the task-positive network, such as lateral prefrontal and parietal networks, reflecting the deactivation of the latter network during the task execution [60]. However, the controversies of this kind of anti-correlation network organization were found among a number of studies [61], [62] due to the high variability of DMN and task-positive network, which might reflect task-related or task-unrelated neural activity. Therefore, it might be not necessary to suggest S2 as a task-relevant connectivity state.

S3 showed strong connections within the bilateral prefrontal network as well as across the networks such as DMN, frontoparietal (task-positive) network and other PFC networks. Frontoparietal network has been well recognized as the control and executive network during task performance [63]. Besides, lateral PFC is one of the executive areas involved in the cognitive control of emotion [39], [64]. During the task execution, high across-network connectivity was commonly found due to the integration among the disconnected executive networks.

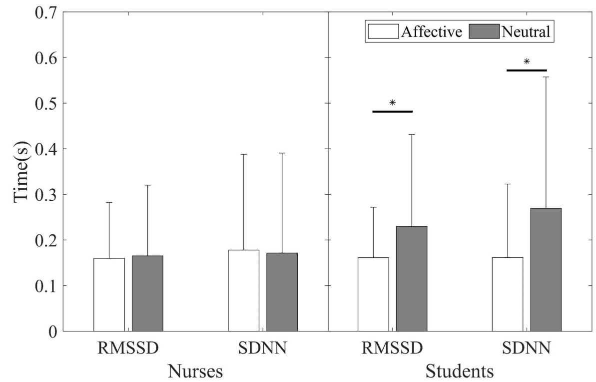

Fig. 7. HRV analysis *RMSSD* and *SDNN* results among nurses and students.

Lastly, S4 demonstrated high connectivity within PFC network. As compared to S3, much less interconnection between brain regions was observed. Yet, as the whole PFC might include executive networks involved in cognitive control, further investigation is required to discard it as a non-task-relevant connectivity state.

B. Dynamic FC Properties

Occurrence probability indicates how frequent a connectivity presents along the recording period, while state transition describes the stability of connectivity during the task performance. The experiment results shows that all subjects tended to remain their connectivity states rather than switching their connectivity states during the task performance. Such phenomenon presented the stability of transition among the subjects. S3, which exhibited the dominant occurrence (40.36%) and significant changes in both occurrence probability and transition stability due to affective task, provided substantial evidence as task-relevant connectivity state. This result is consistent with previous studies [58], [65], which reported increased stability or variability reduction in FC during the engagement of task. Meanwhile, significant reduction occurrence probability and transition stability in S4 was observed. In short, the comparisons of task effect implied a higher susceptibility among the students to both emotional stimuli.

In addition, S1 with the high global connectivity did not show any significant results in both properties among nurses and students due to the emotional effect; on the other hand, S2, which presented an intrinsic network organization, occupied lowest chance of occurrence (overall mean = 12.57%) and did not show any significant result among nurses and students. Therefore, findings show that the connectivity states S1 and S2 might not be suitable to indicate the task-associated connectivity changes due to emotion.

When examined further, the dynamic FC properties provide an insight about the cognitive development state of the nurses and students. As aforementioned, the S1 is task-irrelevant and is at relatively higher level. Such phenomenon might be linked to neuronal noise, which presents during the firing activities of neuronal networks and intensifies during self-organization to permit destabilization and stabilization of neuronal networks [66]. The self-organization is typically characterized by the reduction of local network connectivity and the manifestation of "chaos" in both global and regional brain dynamics, akin to the network characteristics observed in S1. We speculate that the higher level of such neuronal noise for novices (students) is important to facilitate the formation of more optimized task-relevant networks (such as S3 and S4) displayed by the trained minds (nurses). This is evidently with the dominance of S3 for the task by the nurses. Given the largest group differences of occurrence and transition stability in neutral task, this would indicate the different states of cognitive development exhibited by the nurses and students in coping with the emotional stimuli. In other words, the state distribution of nurses might be more optimized than the students', and the state distribution of students transforms and resembles more closely to that of nurses when under the affective condition.

C. Network Characterization

Based on the experimental results, apparent increment of effectiveness in information transmission within global and local networks was observed in the dominant S3 during the affective task. S3 also presented high semi-metricity, indicating higher information sharing among the networks in affective task. In other words, this result highlighted the increasing preference of indirect interconnection among FC networks rather than direct connectivity during affective task. Although S2 possessed the highest E_{local} and SMP, its presence along the task is relatively low as compared to other connectivity states so might not be justified to indicate the task-relevant change. Meanwhile, S1, which was presumed as the global signals, had the poorest information exchange in both global and local network.

D. HRV Analysis

The significant decrements in *RMSSD* and *SDNN* explained the physiological adaptive responses developed among students, evident of the success of inducing negative emotion with the affective stimuli. In contrast, the non-significant change in autonomic nervous system activity strengthens the state distribution of the students to the more optimized distribution as displayed by the nurses.

E. Behavioral Performance

The non-significant changes in the behavioral performance between the nurses and students indicate the same workload undergone by the subject groups while dealing with the decision-making task. Supported by the dynamic FC results, the improved state distribution is likely to translate to the average behavioral performance by the students to reach a higher level, which could be due to the enhanced effort of the compensatory strategies deduced by the attentional control theory [67]. On the other hand, the nurses with the optimized connectivity state distribution, exhibited neither improvement nor impairment of average behavioral performance in both tasks. Hence, this differentiate the emotional sensitivity between the students and nurses.

F. Supervised Classification

According to the emotional state classification results, we identified multiple S3 and S4 of the students to be the input features that produced the highest classification performance and significantly higher than that the nurses. This suggests a higher differential effect of emotion among the students. The second classification comparison shows that the selected features of dynamic FC outperformed the HRV features in terms of area under ROC, prediction accuracy, sensitivity and specificity in recognizing affective stimulus. From the results, we can confirm that task-relevant dynamic FC among students affected under emotional change could be a better predictor as compared to HRV.

Furthermore, it is known that HRV is affected by the emotional state. However, it was not clear to us at the start of this work whether the dynamic FC was a cause or an effect. If the dynamic FC were an effect like HRV, the relationship of classification performance between nurses and students in the dynamic FC would be similar to that of HRV. In contrast, if the dynamic FC were a cause, it would work for the emotion management, i.e., suppressing the emotion and the relationship in the dynamic FC would be different from that of HRV. From Table I, the performance of emotional state classification by both the dynamic FC and HRV for the students was higher than that for the nurses; the performance of emotional state classification by both the dynamic FC and HRV for the nurses was almost 50%, i.e., the dynamic FC is not related with the emotional states in the case of the nurses. These results suggested that the dynamic FC did not originate from the emotion management but a result of emotional state.

G. Limitation

The sample size of nurses was relatively small. Although the result identified that nurses were less sensitive to emotional change than students, the findings might need to be further investigated by increasing the sample size of the nurses. Besides, the age difference between students and nurses could be a confounding factor. Correction factor to the measurements might be required especially when considering nurses who are more than 10 years age older than the students. The implementation of ML also requires a large data set for feature training purpose. The problem of over-fitting might still remain despite our effort to reduce the risk of it.

V. Conclusion

This paper proposed a method for emotional sensitivity detection using fNIRS based dynamic FC and machine learning (clustering and Random Forest algorithms). When assessed with a group of nursing students and registered nurses for a decision-making task, it was found that (1) students were more susceptive to affective stimuli as expected, and (2) dynamic FC provided more differential features than the conventional anxiety measure – HRV in predicting emotional sensitivity. Based on the latter, we proposed a new definition of emotion where brain-based changes should also be considered, in addition to the physiological and behavioral changes in the body. This work illustrated how neuroimaging might help assess the development of emotional sensitivity, and the proposed method demonstrated that the occurrence probability and state transition of dynamic FC as suitable emotional biomarkers. Such biomarkers could be used as the indicators for the development of emotional sensitivity related training required for stressful occupations such as nurses.

Acknowledgment

The authors would like to thank Prof. E. G. Ebenezer, H. Y. Chen (Royal College of Medicine Perak, Universiti Kuala Lumpur) and Y. L. Chan (Centre for Intelligent Signal and Imaging Research, Universiti Teknologi PETRONAS) for the early discussion and the data acquisition.

References

[1] K. R. Scherer, "Appraisal theory," in *Handbook of Cognition and Emotion*, T. Dalgleish and M. Powers, Eds. Hoboken, NJ, USA: Wiley, 1999, pp. 637–663.

[2] B. Wansink and J. Sobal, "Mindless eating: The 200 daily food decisions we overlook," *Environ. Behav.*, vol. 39, no. 1, pp. 106–123, Jan. 2007.

[3] M. J. Duque, C. Turla, and L. Evangelista, "Effects of emotional state on decision making time," *Procedia-Social Behav. Sci.*, vol. 97, pp. 137–146, Nov. 2013.

[4] C. Park, J. Ryu, J. Sohn, and H. Cho, "An emotion expression system for the emotional robot," in *Proc. IEEE Int. Symp. Consum. Electron.*, Jun. 2007, pp. 1–6.

[5] B. Yan *et al.*, "Quantitative identification of major depression based on resting-state dynamic functional connectivity: A machine learning approach," *Frontiers Neurosci.*, vol. 14, pp. 1–13, Mar. 2020.

[6] J. A. Domínguez-Jiménez, K. C. Campo-Landines, J. C. Martínez-Santos, E. J. Delahoz, and S. H. Contreras-Ortiz, "A machine learning model for emotion recognition from physiological signals," *Biomed. Signal Process. Control*, vol. 55, Jan. 2020, Art. no. 101646.

[7] M. Nardelli, G. Valenza, A. Greco, A. Lanata, and E. P. Scilingo, "Recognizing emotions induced by affective sounds through heart rate variability," *IEEE Trans. Affect. Comput.*, vol. 6, no. 4, pp. 385–394, Oct. 2015.

[8] T. C. Ho, E. L. Dennis, P. M. Thompson, and I. H. Gotlib, "Network-based approaches to examining stress in the adolescent brain," *Neurobiol. Stress*, vol. 8, pp. 147–157, Feb. 2018.

[9] R. Sinha, C. M. Lacadie, R. T. Constable, and D. Seo, "Dynamic neural activity during stress signals resilient coping," *Proc. Nat. Acad. Sci. USA*, vol. 113, no. 31, pp. 8837–8842, Aug. 2016.

[10] J. Kim and E. André, "Emotion recognition based on physiological changes in music listening," *IEEE Trans. Pattern Anal. Mach. Intell.*, vol. 30, no. 12, pp. 2067–2083, Dec. 2008.

[11] M. Simões *et al.*, "A novel biomarker of compensatory recruitment of face emotional imagery networks in autism spectrum disorder," *Frontiers Neurosci.*, vol. 12, pp. 1–15, Nov. 2018.

[12] P. A. Kragel and K. S. LaBar, "Multivariate neural biomarkers of emotional states are categorically distinct," *Social Cognit. Affect. Neurosci.*, vol. 10, no. 11, pp. 1437–1448, Nov. 2015.

[13] S. Pryjmachuk, K. Easton, and A. Littlewood, "Nurse education: Factors associated with attrition," *J. Adv. Nursing*, vol. 65, no. 1, pp. 149–160, Jan. 2009.

[14] I. J. Deary, R. Watson, and R. Hogston, "A longitudinal cohort study of burnout and attrition in nursing students," *J. Adv. Nursing*, vol. 43, no. 1, pp. 71–81, Jul. 2003.

[15] E. Lindop, "Individual stress and its relationship to termination of nurse training," *Nurse Educ. Today*, vol. 9, no. 3, pp. 172–179, Jun. 1989.

[16] L. Labrague, "Stress, stressor, and stress responses of student nurses in a government nursing school," *Health Sci. J.*, vol. 7, no. 4, pp. 424–435, 2013.

[17] L. Jan and L. Popescu, "Israel's nursing students' stress sources and coping strategies during their first clinical experience in hospital wards," *Revista Assistenta Sociala*, vol. 4, no. 4, p. 163, 2014.

[18] F. Rafati, E. Nouhi, S. Sabzevari, and N. Dehghan-Nayeri, "Coping strategies of nursing students for dealing with stress in clinical setting: A qualitative study," *Electron. Physician*, vol. 9, no. 12, pp. 6120–6128, Dec. 2017.

[19] W. A. M. Ahmed and B. M. A. Mohammed, "Nursing students' stress and coping strategies during clinical training in KSA," *J. Taibah Univ. Med. Sci.*, vol. 14, no. 2, pp. 116–122, Apr. 2019.

[20] R. W. Carpenter and T. J. Trull, "Components of emotion dysregulation in borderline personality disorder: A review," *Current Psychiatry Rep.*, vol. 15, no. 1, p. 335, Jan. 2013.

[21] J. S. Chong, C.-K. Lu, and T. B. Tang, "Study of emotional state effect on decision making by using fNIRS," in *Proc. IEEE Int. Circuits Syst. Symp. (ICSyS)*, Sep. 2019, pp. 1–4.

[22] C. Chang and G. H. Glover, "Time–frequency dynamics of resting-state brain connectivity measured with fMRI," *NeuroImage*, vol. 50, no. 1, pp. 81–98, Mar. 2010.

[23] M. Mauri *et al.*, "Hemodynamic and behavioral peculiarities in response to emotional stimuli in children with attention deficit hyperactivity disorder: An fNIRS study," *J. Affect. Disorders*, vol. 277, pp. 671–680, Dec. 2020.

[24] S. Sutoko *et al.*, "Exploring attentive task-based connectivity for screening attention deficit/hyperactivity disorder children: A functional near-infrared spectroscopy study," *Neurophotonics*, vol. 6, no. 4, p. 1, Dec. 2019.

[25] F. Waddington *et al.*, "Visual and auditory emotion recognition problems as familial cross-disorder phenomenon in ASD and ADHD," *Eur. Neuropsychopharmacol.*, vol. 28, no. 9, pp. 994–1005, Sep. 2018.

[26] R. C. Oldfield, "The assessment and analysis of handedness: The Edinburgh inventory," *Neuropsychologia*, vol. 9, no. 1, pp. 97–113, 1971.

[27] A. K. Singh, M. Okamoto, H. Dan, V. Jurcak, and I. Dan, "Spatial registration of multichannel multi-subject fNIRS data to MNI space without MRI," *NeuroImage*, vol. 27, no. 4, pp. 842–851, Oct. 2005.

[28] N. Selvaraj, A. Jaryal, J. Santhosh, K. K. Deepak, and S. Anand, "Assessment of heart rate variability derived from finger-tip photoplethysmography as compared to electrocardiography," *J. Med. Eng. Technol.*, vol. 32, no. 6, pp. 479–484, Jan. 2008.

[29] J. Posner, J. A. Russell, and B. S. Peterson, "The circumplex model of affect: An integrative approach to affective neuroscience, cognitive development, and psychopathology," *Develop. Psychopathol.*, vol. 17, no. 3, pp. 715–734, Sep. 2005.

[30] M. M. Bradley and P. J. Lang, "The international affective digitized sounds (2nd edition; IADS-2): Affective ratings of sounds and instruction manual," Univ. Florida, Gainesville, FL, USA, Tech. Rep. B-3, 2007.

[31] N. E. Adams, "Bloom's taxonomy of cognitive learning objectives," *J. Med. Library Assoc.*, vol. 103, no. 3, pp. 152–153, 2015.

[32] B. Molavi and G. A. Dumont, "Wavelet-based motion artifact removal for functional near-infrared spectroscopy," *Physiol. Meas.*, vol. 33, no. 2, pp. 259–270, Feb. 2012.

[33] T. Yamada, S. Umeyama, and K. Matsuda, "Separation of fNIRS signals into functional and systemic components based on differences in hemodynamic modalities," *PLoS ONE*, vol. 7, no. 11, Nov. 2012, Art. no. e50271.

[34] S. Sutoko *et al.*, "Atypical dynamic-connectivity recruitment in attention-deficit/hyperactivity disorder children: An insight into task-based dynamic connectivity through an fNIRS study," *Frontiers Hum. Neurosci.*, vol. 14, p. 3, Jan. 2020.

[35] M. G. Preti, T. A. Bolton, and D. Van De Ville, "The dynamic functional connectome: State-of-the-art and perspectives," *NeuroImage*, vol. 160, pp. 41–54, Oct. 2017.

[36] E. Christiaen *et al.*, "Dynamic functional connectivity and graph theory metrics in a rat model of temporal lobe epilepsy reveal a preference for brain states with a lower functional connectivity, segregation and integration," *Neurobiol. Disease*, vol. 139, Jun. 2020, Art. no. 104808.

[37] Y. Xia *et al.*, "Tracking the dynamic functional connectivity structure of the human brain across the adult lifespan," *Hum. Brain Mapping*, vol. 40, no. 3, pp. 717–728, Feb. 2019.

[38] M. De La Iglesia-Vaya, J. Molina-Mateo, M. J. Escarti-Fabra, A. S. Kanaan, and L. Martí-Bonmatí, "Brain connections—Resting state fMRI functional connectivity," in *Novel Frontiers of Advanced Neuroimaging*, K. N. Fountas, Ed. Rijeka, Croatia: InTech, 2013, ch. 3, pp. 51–66, doi: 10.5772/52273.

[39] M. Uchida *et al.*, "Emotion regulation ability varies in relation to intrinsic functional brain architecture," *Social Cognit. Affect. Neurosci.*, vol. 10, no. 12, pp. 1738–1748, Dec. 2015.

[40] V. Latora and M. Marchiori, "Economic small-world behavior in weighted networks," *Eur. Phys. J. B-Condens. Matter Complex Syst.*, vol. 32, no. 2, pp. 249–263, Mar. 2003.

[41] M. Rubinov and O. Sporns, "Complex network measures of brain connectivity: Uses and interpretations," *NeuroImage*, vol. 52, no. 3, pp. 1059–1069, Sep. 2010.

[42] K. A. Garrison *et al.*, "Functional MRI preprocessing in lesioned brains: Manual versus automated region of interest analysis," *Frontiers Neurol.*, vol. 6, p. 196, Sep. 2015.

[43] S. Achard and E. Bullmore, "Efficiency and cost of economical brain functional networks," *PLoS Comput. Biol.*, vol. 3, no. 2, pp. 0174–0183, 2007.

[44] V. Latora and M. Marchiori, "Efficient behavior of small-world networks," *Phys. Rev. Lett.*, vol. 87, no. 19, Oct. 2001, Art. no. 198701.

[45] T. Simas *et al.*, "Semi-metric topology of the human connectome: Sensitivity and specificity to autism and major depressive disorder," *PLoS ONE*, vol. 10, no. 8, Aug. 2015, Art. no. e0136388.

[46] T. Simas and L. M. Rocha, "Distance closures on complex networks," *Netw. Sci.*, vol. 3, no. 2, pp. 227–268, Jun. 2015.

[47] D. B. Johnson, "Efficient algorithms for shortest paths in sparse networks," *J. ACM*, vol. 24, no. 1, pp. 1–13, Jan. 1977.

[48] M. E. Bartholomew, C. M. Yee, W. Heller, G. A. Miller, and J. M. Spielberg, "Reconfiguration of brain networks supporting inhibition of emotional challenge," *NeuroImage*, vol. 186, pp. 350–357, Sep. 2018.

[49] B. T. Dunkley, S. M. Wong, R. Jetly, J. K. Wong, and M. J. Taylor, "Post-traumatic stress disorder and chronic hyperconnectivity in emotional processing," *NeuroImage, Clin.*, vol. 20, pp. 197–204, Jan. 2018.

[50] C. Kamarajan *et al.*, "Random forest classification of alcohol use disorder using EEG source functional connectivity, neuropsychological functioning, and impulsivity measures," *Behav. Sci.*, vol. 10, no. 3, p. 62, Mar. 2020.

[51] M. Fratello *et al.*, "Multi-view ensemble classification of brain connectivity images for neurodegeneration type discrimination," *Neuroinformatics*, vol. 15, no. 2, pp. 199–213, Apr. 2017.

[52] J. M. Campbell *et al.*, "Pharmacologically informed machine learning approach for identifying pathological states of unconsciousness via resting-state fMRI," *NeuroImage*, vol. 206, Feb. 2020, Art. no. 116316.

[53] M. Vollmer, "A robust, simple and reliable measure of heart rate variability using relative RR intervals," *Comput. Cardiol.*, vol. 42, no. 6, pp. 609–612, 2015.

[54] J. Pan and W. J. Tompkins, "A real-time QRS detection algorithm," *IEEE Trans. Biomed. Eng.*, vol. BME-32, no. 3, pp. 230–236, Mar. 1985.

[55] Y. Benjamini and Y. Hochberg, "Controlling the false discovery rate: A practical and powerful approach to multiple testing," *J. Roy. Stat. Soc., B, Methodol.*, vol. 57, no. 1, pp. 289–300, Jan. 1995.

[56] H. Delgado, X. Anguera, C. Fredouille, and J. Serrano, "Novel clustering selection criterion for fast binary key speaker diarization," in *Proc. INTERSPEECH*, 2015, pp. 3091–3095.

[57] T. T. Liu, A. Nalci, and M. Falahpour, "The global signal in fMRI: Nuisance or information?" *NeuroImage*, vol. 150, pp. 213–229, Apr. 2017.

[58] J. Gonzalez-Castillo and P. A. Bandettini, "Task-based dynamic functional connectivity: Recent findings and open questions," *NeuroImage*, vol. 180, pp. 526–533, Oct. 2018.

[59] J. E. Chen, G. H. Glover, M. D. Greicius, and C. Chang, "Dissociated patterns of anti-correlations with dorsal and ventral default-mode networks at rest," *Hum. Brain Mapping*, vol. 38, no. 5, pp. 2454–2465, May 2017.

[60] M. D. Fox, A. Z. Snyder, J. L. Vincent, M. Corbetta, D. C. Van Essen, and M. E. Raichle, "The human brain is intrinsically organized into dynamic, anticorrelated functional networks," *Proc. Nat. Acad. Sci. USA*, vol. 102, no. 27, pp. 9673–9678, 2005.

[61] X. Di and B. B. Biswal, "Modulatory interactions between the default mode network and task positive networks in resting-state," *PeerJ*, vol. 2, p. e367, May 2014.

[62] K. Murphy, R. M. Birn, D. A. Handwerker, T. B. Jones, and P. A. Bandettini, "The impact of global signal regression on resting state correlations: Are anti-correlated networks introduced?" *NeuroImage*, vol. 44, no. 3, pp. 893–905, Feb. 2009.

[63] M. W. Cole, G. Repovš, and A. Anticevic, "The frontoparietal control system: A central role in mental health," *Neuroscientist*, vol. 20, no. 6, pp. 652–664, 2014.

[64] F. Dolcos, A. D. Iordan, and S. Dolcos, "Neural correlates of emotion—Cognition interactions: A review of evidence from brain imaging investigations," *J. Cognit. Psychol.*, vol. 23, no. 6, pp. 669–694, Sep. 2011.

[65] A. Elton and W. Gao, "Task-related modulation of functional connectivity variability and its behavioral correlations," *Hum. Brain Mapping*, vol. 36, no. 8, pp. 3260–3272, Aug. 2015.

[66] D. Serletis, O. C. Zalay, T. A. Valiante, B. L. Bardakjian, and P. L. Carlen, "Complexity in neuronal noise depends on network interconnectivity," *Ann. Biomed. Eng.*, vol. 39, no. 6, pp. 1768–1778, Jun. 2011.

[67] M. W. Eysenck, N. Derakshan, R. Santos, and M. G. Calvo, "Anxiety and cognitive performance: Attentional control theory," *Emotion*, vol. 7, no. 2, pp. 336–353, 2007.